Spin-polarized electronic structure for the layered two-dimensional $[Fe^{II}(TCNE)(NCMe)_2][Fe^{III}Cl_4]$ organic-based magnet

William W. Shum,[1] Arthur J. Epstein,[2] and Joel S. Miller[1]
[1]*Department of Chemistry, University of Utah, Salt Lake City, Utah 84112-0850, USA*
[2]*Department of Physics and Department of Chemistry, The Ohio State University, Columbus, Ohio 43217, USA*
(Received 20 May 2009; published 7 August 2009)

The results of first-principles density-functional theory and the local-spin-density approximation [L(S)DA] with a Hubbard Coulombic U and projector-augmented wave method electronic-structure calculations for the layered two-dimensional organic-based magnet $[Fe^{II}(TCNE)(NCMe)_2][Fe^{III}Cl_4]$ are reported. The L(S)DA $+U$ method accounted for the on-site Coulomb interaction between the Fe^{II} and μ_4-$[TCNE]^{\bullet-}$ ions. The results from the spin-polarized calculations are in agreement with the antiferromagnetically coupled ferrimagnetic ground state. The magnetic moments for Fe^{II} and $[TCNE]^{\bullet-}$ are 3.70 and 0.27 μ_B, respectively, which are reduced from the sum of the isolated ions (4 and 1 μ_B, respectively) due to antiferromagnetic coupling, which are in accord with molecular-cluster model calculations. Spin-polarized partial density-of-states calculations reveal strongly spin-polarized $Fe^{II}[TCNE]^{\bullet-}$ conduction and valence bands. The highest majority band primarily consists of a Fe^{II} d_{xz}-based band with hybridization (~33%) by a $[TCNE]^{\bullet-}$ p band at 2.60 eV below the Fermi level (E_F), and the highest minority band primarily consists of a $[TCNE]^{\bullet-}$ p band with hybridization (~40%) by Fe^{II} d bands at 0.09 eV below E_F, and the materials is an insulator.

DOI: 10.1103/PhysRevB.80.064403 PACS number(s): 75.25.+z, 71.15.Mb, 71.27.+a, 75.50.Xx

I. INTRODUCTION

In the last few decades, organic-based materials have become an alternative to inorganic solids,[1] due to their controllable properties, especially in combination with other technologically important electrical and optical properties.[2] $V[TCNE]_x \cdot zCH_2Cl_2$ (TCNE=tetracyanoethylene; $x \sim 2$; $z \sim 0.5$) is a room temperature ($T_c \sim 125$ °C) organic-based magnet formed from the reaction of TCNE and $V(C_6H_6)_2$ (Ref. 3) or $V(CO)_6$ (Refs. 3 and 4) in solution or in by chemical vapor deposition.[5] It is a semiconductor with a conductivity approaching 10^{-2} S/cm at room temperature.[6] In addition, magnetotransport studies reveal that electrons in both of the valence and conduction bands of $V[TCNE]_x \cdot zCH_2Cl_2$ are spin polarized,[7] suggestive of "spintronic" applications.[8]

In addition to $V[TCNE]_x$, $M[TCNE]_x \cdot zCH_2Cl_2$ (M=Mn, Fe, Co, and Ni) magnetically order as high as 100 K.[9] More recently, $[Fe(TCNE)(NCMe)_2][FeCl_4]$ has been reported to have a 90 K T_c.[10] While the study of $V[TCNE]_x$ has been limited by the paucity of structural information beyond the V-N distance,[11] both $Fe[TCNE]_x \cdot zCH_2Cl_2$ (Ref. 9) and $[Fe(TCNE)(NCMe)_2][FeCl_4]$ have been structurally characterized.[10] Their study will provide deeper insight into the electronic, electrical, and magnetic properties of this family of molecule-based magnets enabling a better understanding of $V(TCNE)_x$. Both $Fe[TCNE]_x \cdot zCH_2Cl_2$ (Ref. 9) and $[Fe(TCNE)(NCMe)_2][FeCl_4]$ (Ref. 10) possess a layered magnetic structure, with the layers separated by MeCN ligands for the latter (Fig. 1), and bridged by diamagnetic μ_4-$[C_4(CN)_8]^{2-}$ for the former. The layered structure for $[Fe(TCNE)(NCMe)_2][FeCl_4]$ consists of Fe^{II} bonded to four μ_4-$[TCNE]^{\bullet-}$ and is a ferrimagnet due to antiferromagnetic coupling among the high spin $S=2$ Fe^{II} with the $S=1/2$ μ_4-$[TCNE]^{\bullet-}$. In addition, two MeCN ligands are bonded perpendicular to Fe^{II}-based undulating plane giving a distorted local D_{4h} environment for each Fe^{II} site. The $S=5/2$ $[Fe^{III}Cl_4]^-$ counter anion resides between the layers but does not contribute to the magnetic ordering.[10,12] Given that the $[Fe(TCNE)(NCMe)_2]^+$ orders as a ferrimagnet, it should exhibit spin polarization below the critical temperature[13] and a spin-polarized electron structure has been experimentally observed for $[Fe(TCNE)(NCMe)_2][FeCl_4]$ (Ref. 14) but it is an insulator.[15]

To complement the experimental observation of spin polarized for $[Fe(TCNE)(NCMe)_2][FeCl_4]$ and extend the preliminary computational study, its electronic structure is herein computationally investigated by including a Hubbard U term to account for the on-site Coulomb interactions. While several inorganic materials exhibiting spin polarization have been widely studied, e.g., CrO_2,[16] $[Fe^{II}(TCNE)(NCMe)_2][Fe^{III}Cl_4]$ is the first spin-polarized

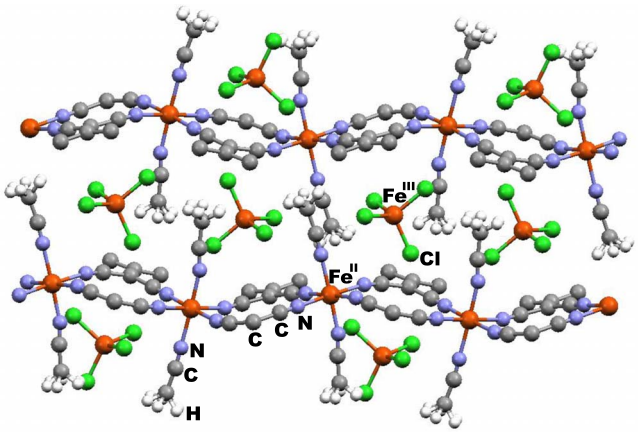

FIG. 1. (Color online) Crystal structure of $[Fe(TCNE)(NCMe)_2][FeCl_4]$ (H, white; C, gray; N, blue, Cl, green, and Fe, red) (Ref. 10). Due to structural disorder each methyl groups displays 6 H atoms.

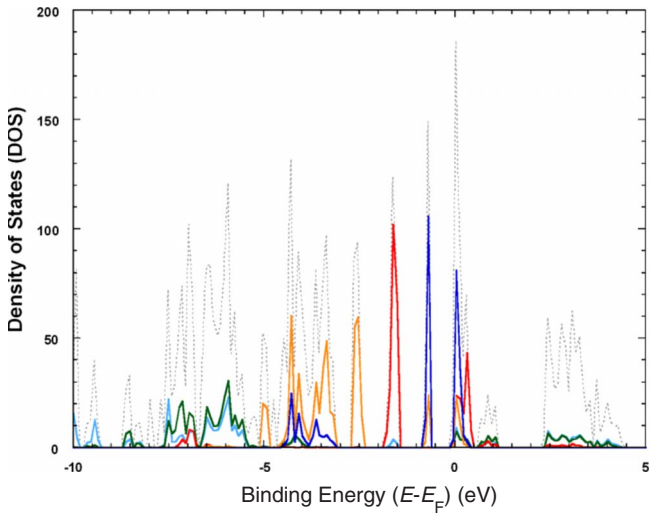

FIG. 2. (Color online) Partial density of states from LDA PAW calculation. Total DOS (—); $[TCNE]^{\bullet-}$ C p (—); $[TCNE]^{\bullet-}$ N p (—); Cl p (—); Fe^{II} d (—); and Fe^{III} d (—).

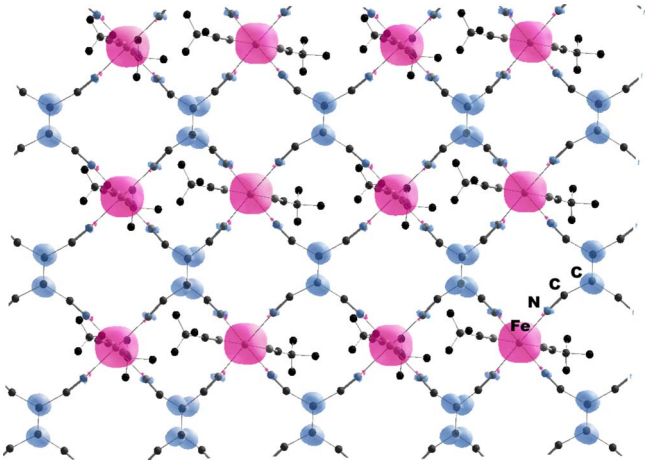

FIG. 3. (Color online) Spin-density isosurface of a ferrimagnetic layer of $[Fe^{II}(TCNE^{\bullet-})(NCMe)_2]^+$ calculated by the L(S)DA+U method. The red isosurface indicates the spin-up electron density; the blue isosurface indicates the spin-down electron density. All atoms are black.

organic-based material with structural information to be computationally investigated in detail.[14] With the investigation of potential for spintronics applications, this will be a promising prototype for future organic-spin-based electronics and also provide further insight into $V(TCNE)_x$.

II. COMPUTATIONAL DETAILS

All calculations were performed using the density-function method (DFT).[17] The Kohn-Sham equations were solved self-consistently using structural parameters fixed at their experimental values.[10] The local-density approximation (LDA) was used with projector-augmented wave (PAW) as plane-wave basis functions.[18] The PAW potentials for Fe were generated from the $[Ar]3d^64s^2$ atomic configuration and the $3d$ and $4s$ electrons were treated as valence electrons. The atomic potentials for H, C, and N were generated from the $1s^1$, $[He]2s^22p^2$, and $[He]2s^22p^3$ atomic configurations, respectively. The $2s$ and $2p$ electrons were considered as valence electrons for C and N. The plane-wave energy cutoff was set at 350 eV and $8\times8\times8$ k-point mesh was generated according to the Γ-centered Monkhorst-Pack scheme to sample the Brillouin zone[19] (resulting in 125 k points in the irreducible Brillouin zone). For spin-polarized calculation, the L(S)DA+U method[20] was used. The Hubbard U was included to account for the on-site Coulomb interactions. We adopted the simplified rotationally invariant approach formulated by Dudarev *et al.*[21] The total energy can be summarized by the following expression:

$$E^{\mathrm{L(S)DA}+U} = E^{\mathrm{L(S)DA}} + \frac{U-J}{2}\sum_{\sigma}\left[\left(\sum_{m} n^{\sigma}_{m,m}\right) - \left(\sum_{m,m'} n^{\sigma}_{m,m'} n^{\sigma}_{m',m}\right)\right], \quad (1)$$

where U and J are the spherically averaged matrix elements of the screened Coulomb electron-electron interactions; U is the effective on-site Coulomb interaction parameter and J is the effective on-site exchange interaction parameter (in this approach, only $U-J$ is meaningful, not U and J separately). n is the on-site occupation matrix obtained by projection of the wave function, m is the on-site orbitals for (e.g., on-site interaction for d orbitals, m or $m'=-2, -1, 0, 1,$ and 2), and σ is the spin (1 or −1). The values of U and J for Fe, C, and N were adopted from Ref. 22. The initial guess for the calculation included the difference between the number of spin-up and spin-down electrons (i.e., 3) for each antiferromagnetically coupled Fe(TCNE) moiety. Since Fe^{II} is high spin ($S=2$) and $[TCNE]^{\bullet-}$ is $S=1/2$, the initial guess was accounted for that when calculating magnetization (see supporting information).

Molecular-cluster model linear combination of atomic orbitals (LCAO) calculations were performed using the DFT method with all-electron Gaussian-type orbital.[23] An unrestricted hybrid DFT, the Becke's three parameters with Lee-Yang-Parr correlation function,[24] was used with a 6-31+ $+g(d,p)$ basis set for H, C, and N, and an Ahlrich's triple ζ valence[25] basis set for Fe^{II}. Methyl groups were substituted by H for simplicity and to enforce D_{2h} symmetry. A high-spin wave function of the cluster model was initially obtained. This was followed by a calculation utilizing the broken-symmetry method (BS-DFT) to see if it has an antiferromagnetic ground state.[26]

III. RESULTS AND DISCUSSION

The density of states (DOS) of crystalline **1** calculated by LDA method is shown in Fig. 2. The partial density of states (PDOS) of the p orbitals of $[TCNE]^{\bullet-}$, Cl^-, and the d orbitals of Fe^{II} and Fe^{III} are shown along with the total DOS. The highest-occupied Fe^{II} and Fe^{III} d bands are at 1.52 and 0.69 eV below the Fermi level (E_F), respectively, and both d bands are hybridized by $[TCNE]^{\bullet-}$ and Cl^- p bands. Since the LDA calculation is nonspin polarized and thus does not

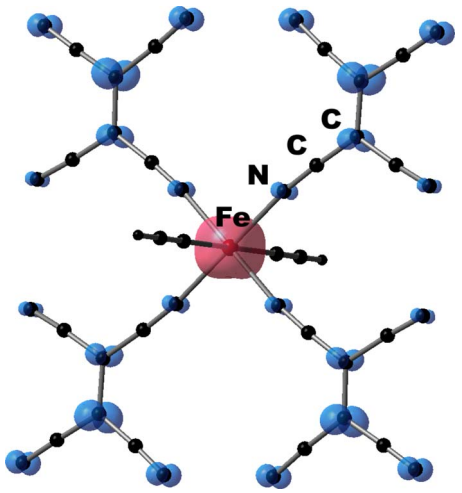

FIG. 4. (Color online) Spin density of an antiferromagnetic Fe^{II}-$TCNE^{\bullet-}$ fragment calculated by the LCAO molecular-cluster model. The red isosurface indicates the spin-up electron density and the blue isosurface indicates the spin-down electron density. All atoms are black.

distinguish between low and high spin for Fe^{II} ($S=2$) and Fe^{III} ($S=5/2$). Also, both Fe^{II} and $[TCNE]^{\bullet-}$ exhibit strong Coulomb interaction from theoretical and experimental results,[22] therefore a Hubbard U is included to account for the Coulomb term in the spin-polarized calculations.

As the paramagnetic $[Fe^{III}Cl_4]^-$ counter anion does not contribute to magnetic ordering,[12] the spin-polarized calculations were simplified by removing it and focusing only on the magnetic layers. The calculations for both one and two layers of $[Fe^{II}(TCNE)(NCMe)_2]^+$ take into account the differences between spin-up and spin-down electrons for $Fe^{II}(TCNE^{\bullet-})$, and the initial magnetic moments, to ensure Fe^{II} high spin $S=2$ and $[TCNE]^{\bullet-}$ $S=1/2$. Furthermore, both antiferromagnetic and ferromagnetic interactions between Fe^{II} and $[TCNE]^{\bullet-}$ were evaluated.

The L(S)DA+U calculation of two layers per unit cell showed no sign of interaction between the layers and this is ascribed to the large interlayer separation (~8.5 Å). In the calculation for single layer per unit cell, the antiferromagnetic ground state between Fe^{II} and $[TCNE]^{\bullet-}$ were found to be lower in energy than the ferromagnetic ground state, in agreement with previous experimental results.[10] This calculation gives magnetic moments of 3.70 μ_B for Fe^{II} and 0.27 μ_B for $[TCNE]^{\bullet-}$ (average 0.111, 0.011, 0.013 μ_B for sp^2 C, sp C, and N, respectively) or 3.43 μ_B/FeTCNE, due to antiferromagnetic coupling, Fig. 3. Note that the spin only, uncoupled moments are expected to be higher for both $[TCNE]^{\bullet-}$ (1 μ_B) and Fe^{II} (4 μ_B assuming the Landé g value is 2.0023). However, since spin-orbit coupling was expected for high-spin Fe^{II}, its magnetic moment should exceed 4 μ_B.

In order to understand the lower than expected magnetic moments, a thorough qualitative analysis utilizing molecular-cluster model LCAO calculations were executed to provide further insight into the antiferromagnetic interaction[26,27] between Fe^{II} and $[TCNE]^{\bullet-}$. An antiferromagnetic ground state obtained by BS-DFT method showed the spin density of

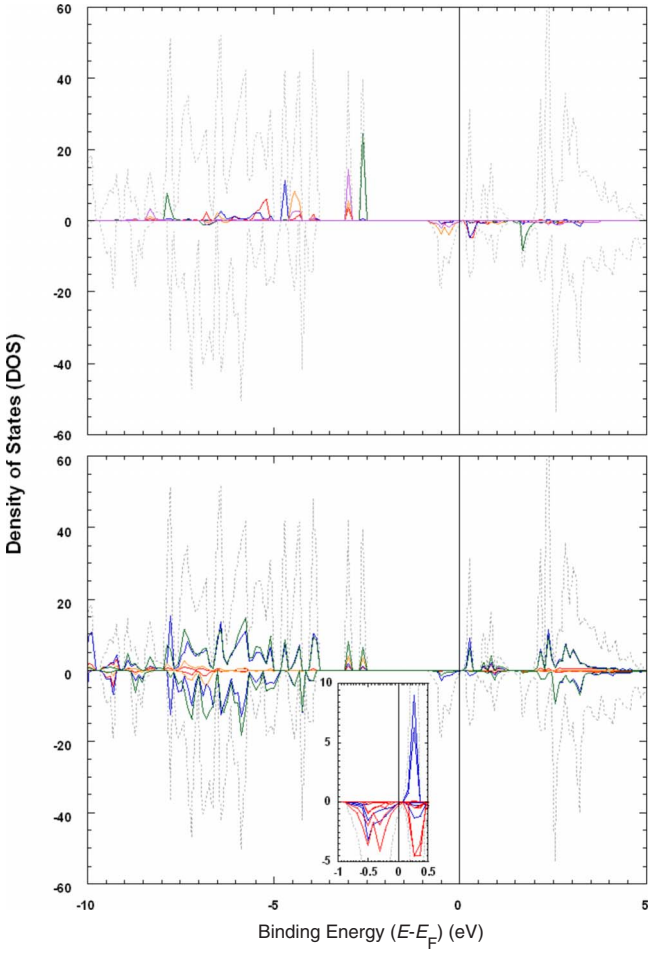

FIG. 5. (Color online) Spin-polarized partial density of states of layer $[Fe^{II}(TCNE^{\bullet-})(NCMe)_2]^+$. Total DOS (—); top: Fe^{II} d_{xy} orbital (—); d_{yz} (—); d_{z^2} (—); d_{xz} (—); $d_{x^2-y^2}$ (—); bottom: TCNE C s (—); p (—) and N s (—); p (—). Inset: all Fe^{II} bands (—), all $[TCNE]^{\bullet-}$ bands (—).

$[TCNE]^{\bullet-}$ is opposite to that of Fe^{II}, Fig. 4. Moreover, the spin density on the C-CN fragment connected to Fe^{II} is reduced, partly due to the ligand-to-metal charge transfer in the antiferromagnetic ground state, as was previously observed for $Mn^{II}(C_5H_5)(CO)_2(TCNE^{\bullet-})$.[28] A natural bond orbital (NBO) (Ref. 29) analysis (Table I) showed Fe^{II} has a spin electron density of 3.65 unpaired, spin-up (α) electrons ($S=1.83$); the unbonded C(6)C(8)N(10) fragment has 0.343 unpaired, spin-down (β), 0.066 α, and 0.178 β electrons, respectively, and the C(4)C(3)N(2) fragment, connected to Fe^{II}, has 0.011, 0.093, and 0.108 β electrons, respectively. The spin electron density on the central, C(4) and C(6), carbons will be further reduced when all CNs are bonded to additional Fe^{II} ions, as occurs within the layers. If the total spin density is based on the NBO value of Fe^{II}-bonded N(2)C(3)C(4), the total spin electron density will be −0.805 unpaired electron (~0.4 μ_B spin down). Furthermore, the spin electron density of the central C(4) is higher than in the case of a $Fe^{II}(TCNE^{\bullet-})$ layer. A lower spin-density value is expected for C(4) as C(5)N(11) is bonded to an additional Fe^{II} (in a periodic boundary condition), due to the antiferromagnetic interaction. The reduced electron density on C(3)

TABLE I. NBO analysis of Fe^{II}-$[TCNE]^{\bullet-}$ (showed only one $[TCNE]^{\bullet-}$ per Fe since all four are equivalent, unit in number of electron).

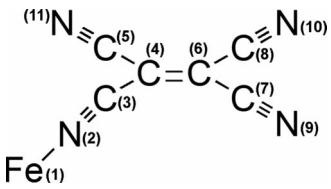

Atom	Natural charge	Core	Valence	Rydberg	Total	Spin density
Fe1	1.47843	17.99318	6.51283	0.01556	24.52157	3.65000
N2	−0.54253	1.99928	5.50774	0.03551	7.54253	−0.09304
C3	0.41633	1.99906	3.55956	0.02505	5.58367	−0.01095
C4	−0.32564	1.99865	4.30656	0.02043	6.32564	−0.19427
C5	0.26875	1.99922	3.69856	0.03347	5.73125	0.03753
C6	−0.26658	1.99855	4.24950	0.01853	6.26658	−0.34334
C7	0.25591	1.99923	3.71206	0.03280	5.74409	0.06909
C8	0.28243	1.99925	3.68506	0.03326	5.71757	0.06565
N9	−0.30881	1.99955	5.28837	0.02089	7.30881	−0.17519
N10	−0.35554	1.99954	5.33516	0.02084	7.35554	−0.17799
N11	−0.31401	1.99954	5.29308	0.02139	7.31401	−0.10104

also could be a factor of the low conductivity. This analysis is consistent with the magnetic moments for the $Fe^{II}(TCNE^{\bullet-})$ unit obtained from L(S)DA+U-based calculations.[30]

The calculated spin-polarized partial density of states shows that a $[Fe^{II}(TCNE^{\bullet-})(NCMe)_2]^+$ single layer to be strongly polarized at both the valence (0 to −6 eV with respect to E_F) and conduction bands (0 to +2.5 eV with respect to E_F), Fig. 5. The highest-occupied molecular orbital (HOMO) majority band (spin up) and minority band (spin down) are found to be at 2.60 and 0.09 eV, respectively, below E_F. The spin-up HOMO is primarily composed of the Fe^{II} d_{xz} orbital (~33%) that is hybridized by the $[TCNE]^{\bullet-}$ p orbitals and the spin-down HOMO is primarily composed of p orbitals from the $[TCNE]^{\bullet-}$ that are hybridized by (~40%) the Fe^{II} d orbitals. The inset in Fig. 5 shows the $[TCNE]^{\bullet-}$ p bands cross the Fermi level without an obvious band gap. This highest-occupied $[TCNE]^{\bullet-}$ p band was contributed from the $[TCNE]^{\bullet-}$ π^* orbitals. The $\pi^*-\pi^*+U$ splitting is about 0.8 eV, as a result of the Coulomb interaction (in which splits the π^* band into π^* and π^*+U bands). The $\pi^*-\pi^*+U$ splitting in $Fe^{II}[TCNE]^{\bullet-}$ is smaller than in $V^{II}[TCNE]^{\bullet-}$ and the Fe^{II} d bands (both e_g and t_{2g}) are lower in energy than the V^{II} d bands (t_{2g}). Furthermore, modification of $[TCNE]^{\bullet-}$ $U-J$ parameters from 0 to 4 eV does not show any significant change in the $\pi^*-\pi^*+U$ splitting. Thus, the L(S)DA+U calculations for a single layer of $[Fe^{II}(TCNE^{\bullet-})(NCMe)_2]^+$ predicted the Fe^{II} d bands and the $[TCNE]^{\bullet-}$ p bands to be strongly spin polarized. The calculated multiple Fe^{II} d bands (~−2.5 to −6 eV with respect to E_F) were a result of the distorted local D_{4h} environment. While the e_g bands (~−2.5 to −3 eV) are appeared to be localized in the calculated results, the t_{2g} bands (~−3.6 to −6 eV) show indication of electron dispersion and are mixing with the $[TCNE]^{\bullet-}$ π orbitals. This result was summarized with a schematic shown in Fig. 6.

IV. CONCLUSION

L(S)DA+U DFT calculations on $[Fe^{II}(TCNE)(NCMe)_2][Fe^{III}Cl_4]$ confirm the ferrimagnetic ground state for single layer $[Fe^{II}(TCNE^{\bullet-})(NCMe)_2]^+$, with antiferromagnetic-coupled magnetic moments of 3.70 and 0.27 μ_B for Fe^{II} and $[TCNE]^{\bullet-}$, respectively. Hence, inclusion of the Hubbard U Coulomb term accounts for the spins and magnetic moment that were not accounted for in the

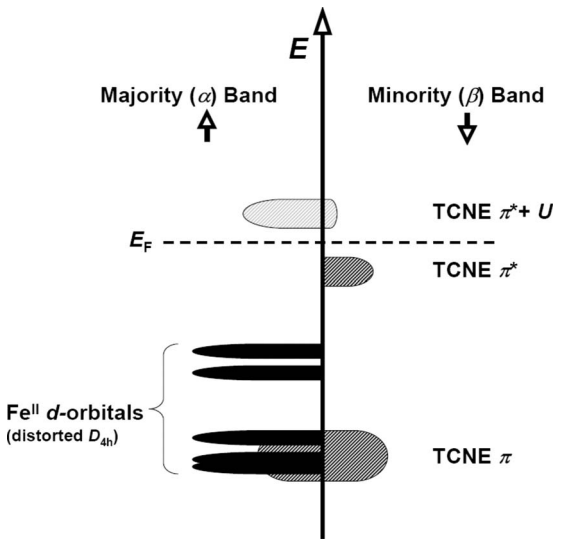

FIG. 6. Schematic illustration of spin-polarized density of states for $[Fe^{II}(TCNE^{\bullet-})]^+$.

preliminary calculation. Furthermore, the highest band arises primarily $[TCNE]^{\bullet -}$ based, not Fe^{II} based.

Analysis of the PDOS reveals that both the valence and conduction bands are spin polarized and has minority bands near the Fermi level. The $[TCNE]^{\bullet -}$ p orbitals are found to be the highest-occupied minority bands 0.09 eV under the Fermi level with hybridization by the Fe^{II} d bands, with Fe^{II} d band 2.60 eV under the Fermi level with hybridization by the $[TCNE]^{\bullet}$ p bands. Below the critical temperature, $[Fe^{II}(TCNE)(NCMe)_2][Fe^{III}Cl_4]$ should exhibit spin-polarization behavior. This layered ferrimagnetic material, however, is found to be an insulator,[15] which could be a result of the reduced electron density of the nitriles due to the antiferromagnetic interactions.

ACKNOWLEDGMENTS

We appreciate the helpful discussions with Anthony N. Caruso (University of Missouri-Kansas City) and Konstantin I. Pokhodnya (North Dakota State University), and the continued partial support by the DOE Division of Material Science (Grants No. DE-FG03-93ER45504 and No. DE-FG02-01ER4593). W.W.S. would like to acknowledge the computational allocation generously provided by the National Institutes of Health (Grant No. NCRR 1 S10 RR17214-01) on the Arches Metacluster administered by the University of Utah Center for high performance computing. Special thanks need to be given to Thanh Truong for making the VASP code available to us and Martin Cuma for technical assistance.

[1] J. S. Miller, Adv. Mater. **2**, 98 (1990).

[2] V. I. Ovcharenko and R. Z. Sagdeev, Russ. Chem. Rev. **68**, 345 (1999); M. Kinoshita, Philos. Trans. R. Soc. London, Ser. A **357**, 2855 (1999); J. S. Miller and A. J. Epstein, Angew. Chem., Int. Ed. Engl. **33**, 385 (1994); J. S. Miller and A. J. Epstein, Chem. Eng. News **73**, 30 (1995); S. J. Blundell and F. L. Pratt, J. Phys.: Condens. Matter **16**, R771 (2004).

[3] J. M. Manriquez, G. T. Yee, R. S. McLean, A. J. Epstein, and J. S. Miller, Science **252**, 1415 (1991); J. S. Miller and A. J. Epstein, Chem. Commun. (Cambridge) **1998**, 1319.

[4] J. Zhang, J. S. Miller, C. Vazquez, P. Zhou, W. B. Brinckerhoff, and A. J. Epstein, ACS Symp. Ser. **644**, 311 (1996).

[5] K. I. Pokhodnya, A. J. Epstein, and J. S. Miller, Adv. Mater. **12**, 410 (2000); K. I. Pokhodnya, D. Pejakovic, A. J. Epstein, and J. S. Miller, Phys. Rev. B **63**, 174408 (2001).

[6] G. Du, J. Joo, A. J. Epstein, and J. S. Miller, J. Appl. Phys. **73**, 6566 (1993).

[7] C. Tengstedt, M. P. de Jong, A. Kanciurzewska, E. Carlegrim, and M. Fahlman, Phys. Rev. Lett. **96**, 057209 (2006).

[8] V. N. Prigodin, N. P. Raju, K. I. Pokhodnya, J. S. Miller, and A. J. Epstein, Adv. Mater. **14**, 1230 (2002).

[9] J. Zhang, J. Ensling, V. Ksenofontov, P. Gütlich, A. J. Epstein, and J. S. Miller, Angew. Chem., Int. Ed. **37**, 657 (1998).

[10] K. I. Pokhodnya, M. Bonner, J.-H. Her, P. W. Stephens, and J. S. Miller, J. Am. Chem. Soc. **128**, 15592 (2006).

[11] D. Haskel, Z. Islam, J. Lang, C. Kmety, G. Srajer, K. I. Pokhodnya, A. J. Epstein, and J. S. Miller, Phys. Rev. B **70**, 054422 (2004).

[12] J.-W. Yoo, V. N. Prigodin, W. W. Shum, K. I. Pokhodnya, J. S. Miller, and A. J. Epstein, Phys. Rev. Lett. **101**, 197206 (2008).

[13] C. Felser, G. H. Fecher, and B. Balke, Angew. Chem., Int. Ed. **46**, 668 (2007).

[14] A. N. Caruso, K. I. Pokhodnya, W. W. Shum, W. Y. Ching, B. Anderson, M. T. Bremer, E. Vescovo, P. Rulis, A. J. Epstein, and J. S. Miller, Phys. Rev. B **79**, 195202 (2009).

[15] The conductivity is $\leq 10^{-10}$ S/cm, J.-W. Yoo, A. J. Epstein, and J. S. Miller (unpublished).

[16] K. P. Kämper, W. Schmitt, G. Güntherodt, R. J. Gambino, and R. Ruf, Phys. Rev. Lett. **59**, 2788 (1987); R. A. de Groot, F. M. Mueller, P. G. van Engen, and K. H. J. Buschow, *ibid.* **50**, 2024 (1983); L. Chioncel, H. Allmaier, E. Arrigoni, A. Yamasaki, M. Daghofer, M. I. Katsnelson, and A. I. Lichtenstein, Phys. Rev. B **75**, 140406(R) (2007); J. M. Coey and M. Venkatesan, J. Appl. Phys. **91**, 8345 (2002).

[17] P. Hohenberg and W. Kohn, Phys. Rev. **136**, B864 (1964); W. Kohn and L. J. Sham, *ibid.* **140**, A1133 (1965); Vienna ab initio simulation package (VASP) version 4.6. G. Kresse and J. Furthmüller, Comput. Mater. Sci. **6**, 15 (1996); G. Kresse and J. Furthmüller, Phys. Rev. B **54**, 11169 (1996).

[18] P. E. Blöchl, Phys. Rev. B **50**, 17953 (1994).

[19] H. J. Monkhorst and J. D. Pack, Phys. Rev. B **13**, 5188 (1976); G. Kresse and D. Joubert, *ibid.* **59**, 1758 (1999).

[20] I. V. Solovyev, P. H. Dederichs, and V. I. Anisimov, Phys. Rev. B **50**, 16861 (1994); A. B. Shick, A. I. Liechtenstein, and W. E. Pickett, *ibid.* **60**, 10763 (1999).

[21] S. L. Dudarev, G. A. Botton, S. Y. Savrasov, C. J. Humphreys, and A. P. Sutton, Phys. Rev. B **57**, 1505 (1998).

[22] Z. Zhang and S. Satpathy, Phys. Rev. B **44**, 13319 (1991); V. I. Anisimov, I. S. Elfimov, N. Hamada, and K. Terakura, *ibid.* **54**, 4387 (1996); G. Rollmann, P. Entel, A. Rohrbach, and J. Hafner, Phase Transitions **78**, 251 (2005); N. P. Raju, T. Savrin, V. N. Prigodin, K. I. Pokhodnya, J. S. Miller, and A. J. Epstein, J. Appl. Phys. **93**, 6799 (2003); S. K. Khanna, A. A. Bright, A. F. Garito, and A. J. Heeger, Phys. Rev. B **10**, 2139 (1974); A. J. Epstein, S. Etemad, A. F. Garito, and A. J. Heeger, *ibid.* **5**, 952 (1972).

[23] GAUSSIAN 03, Revision C.02, M. J. Frisch, G. W. Trucks, H. B. Schlegel, G. E. Scuseria, M. A. Robb, J. R. Cheeseman, J. A. Montgomery, Jr., T. Vreven, K. N. Kudin, J. C. Burant, J. M. Millam, S. S. Iyengar, J. Tomasi, V. Barone, B. Mennucci, M. Cossi, G. Scalmani, N. Rega, G. A. Petersson, H. Nakatsuji, M. Hada, M. Ehara, K. Toyota, R. Fukuda, J. Hasegawa, M. Ishida, T. Nakajima, Y. Honda, O. Kitao, H. Nakai, M. Klene, X. Li, J. E. Knox, H. P. Hratchian, J. B. Cross, V. Bakken, C. Adamo, J. Jaramillo, R. Gomperts, R. E. Stratmann, O. Yazyev, A. J. Austin, R. Cammi, C. Pomelli, J. W. Ochterski, P. Y. Ayala, K. Morokuma, G. A. Voth, P. Salvador, J. J. Dannenberg, V. G. Zakrzewski, S. Dapprich, A. D. Daniels, M. C. Strain, O. Farkas, D. K. Malick, A. D. Rabuck, K. Raghavachari, J. B. Foresman, J. V. Ortiz, Q. Cui, A. G. Baboul, S. Clifford, J.

Cioslowski, B. B. Stefanov, G. Liu, A. Liashenko, P. Piskorz, I. Komaromi, R. L. Martin, D. J. Fox, T. Keith, M. A. Al-Laham, C. Y. Peng, A. Nanayakkara, M. Challacombe, P. M. W. Gill, B. Johnson, W. Chen, M. W. Wong, C. Gonzalez, and J. A. Pople, Gaussian, Inc., Wallingford, CT, 2004.

[24] A. D. Becke, Phys. Rev. A **38**, 3098 (1988); C. Lee, W. Yang, and R. G. Parr, Phys. Rev. B **37**, 785 (1988); A. D. Becke, J. Chem. Phys. **98**, 5648 (1993).

[25] R. Ditchfield, W. J. Hehre, and J. A. Pople, J. Chem. Phys. **54**, 724 (1971); A. Schafer, C. Huber, and R. J. Ahlrichs, J. Chem. Phys. **100**, 5829 (1994).

[26] L. Noodleman, J. Chem. Phys. **74**, 5737 (1981); L. Noodlemann and E. R. Davidson, Chem. Phys. **109**, 131 (1986).

[27] L. Noodleman, D. A. Case, and A. Aizman, J. Am. Chem. Soc. **110**, 1001 (1988).

[28] J. J. Novoa, J. Ribas-Arino, W. W. Shum, and J. S. Miller, Inorg. Chem. **46**, 103 (2007).

[29] J. E. Carpenter and F. Weinhold, J. Mol. Struct.: THEOCHEM **169**, 41 (1988).

[30] See EPAPS Document No. E-PRBMDO-80-071926 for supplementary materials. For more information on EPAPS, see http://www.aip.org/pubservs/epaps.html.